Electronic Supplementary Material (ESI) for CrystEngComm

Supplementary Information

Microstructural Study for Understanding the Formation Mechanism of Metal-Organic Framework MOF-5

Chunman Zheng, Heather F. Greer, Chang-Yang Chiang, Wuzong Zhou

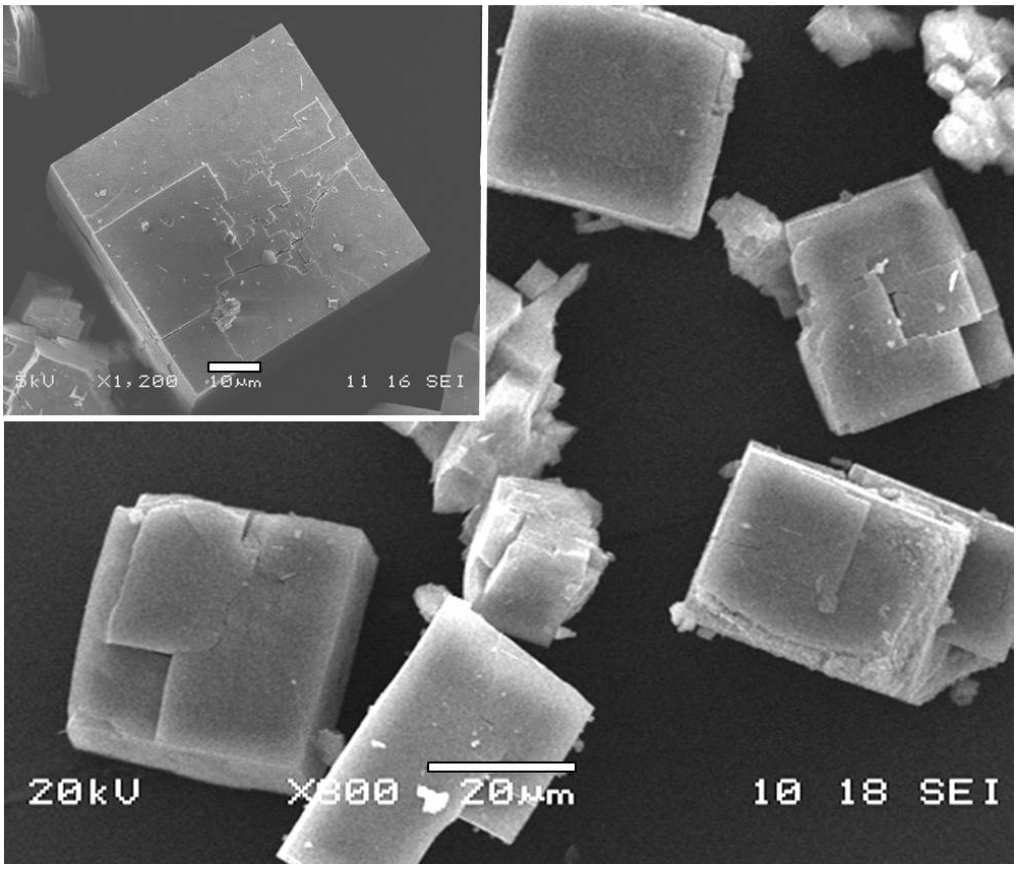

Figure S1. SEM images of MOF-5 crystals recorded from the 36 h sample. The inset is a SEM image of a cube showing an uncompleted surface layer containing many orientated plates, which is commonly observed on the surface of individual crystals.

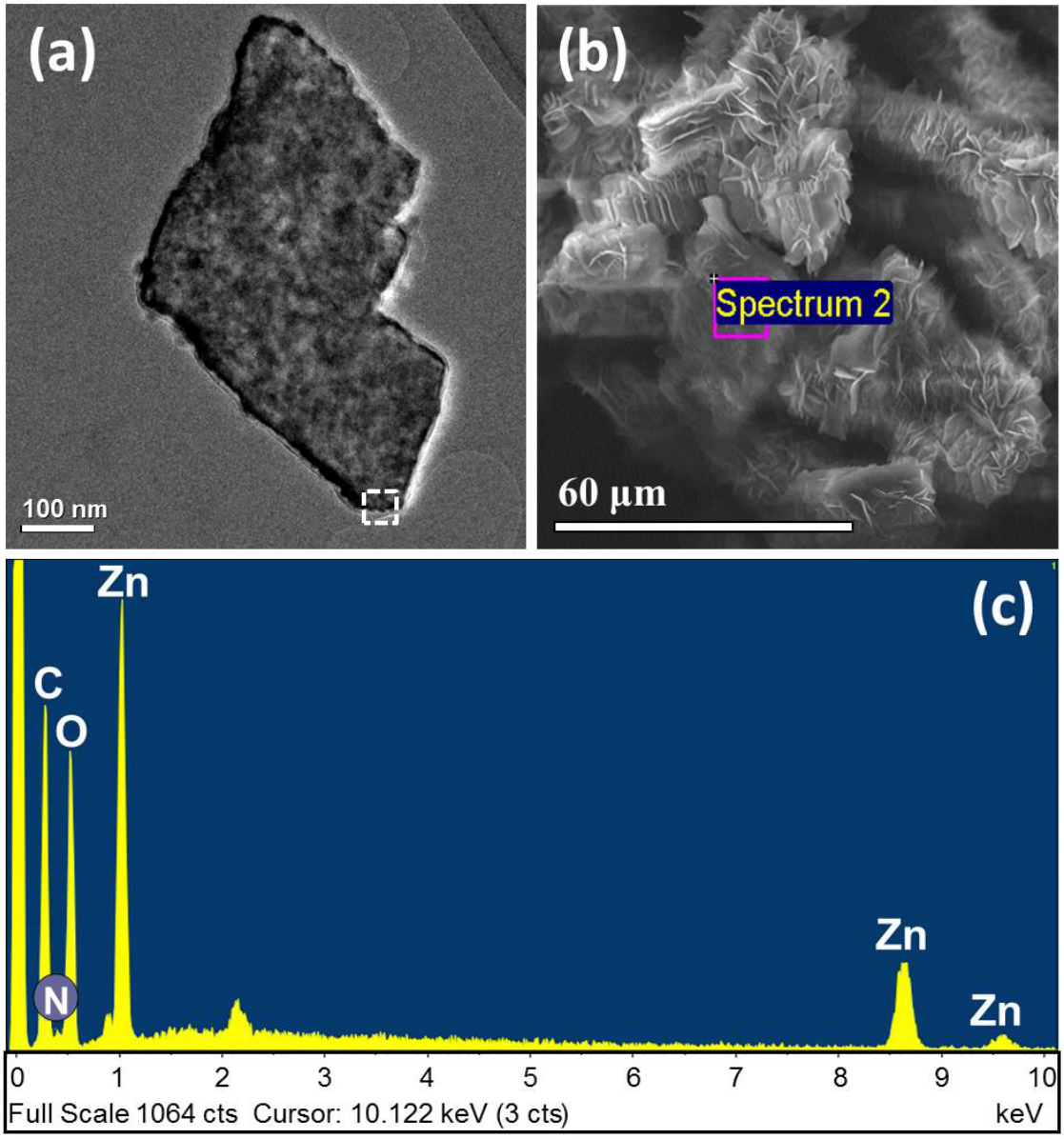

Figure S2. Characterisation of the 2 h sample containing $Zn_5(OH)_8(NO_3)_2 \bullet 2H_2O$ microplates. (a) TEM image of a fragment of a microplate from the 2 h sample, showing that it consists of many nanoplatelets. The HRTEM image in Fig. 1b was recorded from the region marked by a box. (b) SEM image of clusters of microplates. (c) EDX spectrum obtained from the area marked in (b). The peak at about 2.1 KeV is the Au K line from the coating.

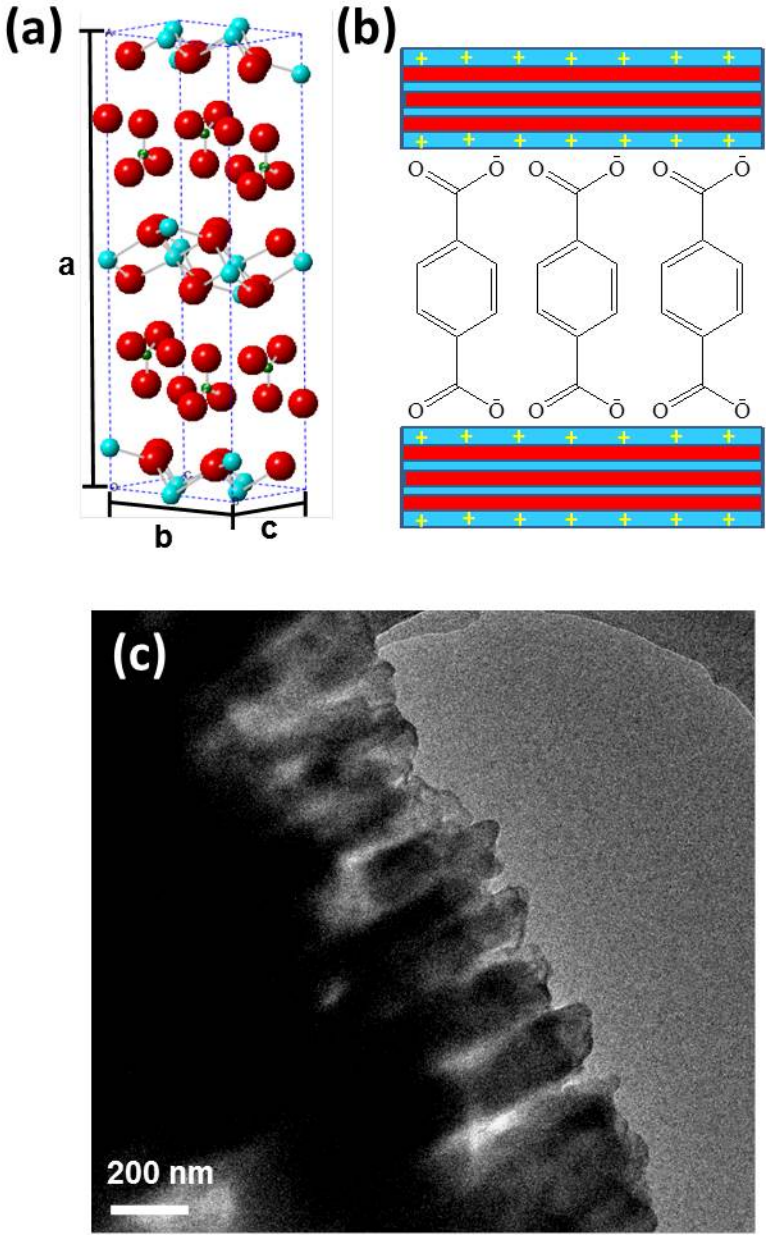

Figure S3. Intercalation of 1,4-BDC molecules into $Zn_5(OH)_8(NO_3)_2 \bullet 2H_2O$. (a) Crystal structure of $Zn_5(OH)_8(NO_3)_2 \bullet 2H_2O$. (b) A model showing the distribution of electric charge in $Zn_5(OH)_8(NO_3)_2 \bullet 2H_2O$ plates and one possible intercalation arrangement of the 1,4-BDC molecules. (c) TEM image of such a layered composite from the 4 h sample, showing the thickness of the microplates and the interplate space.

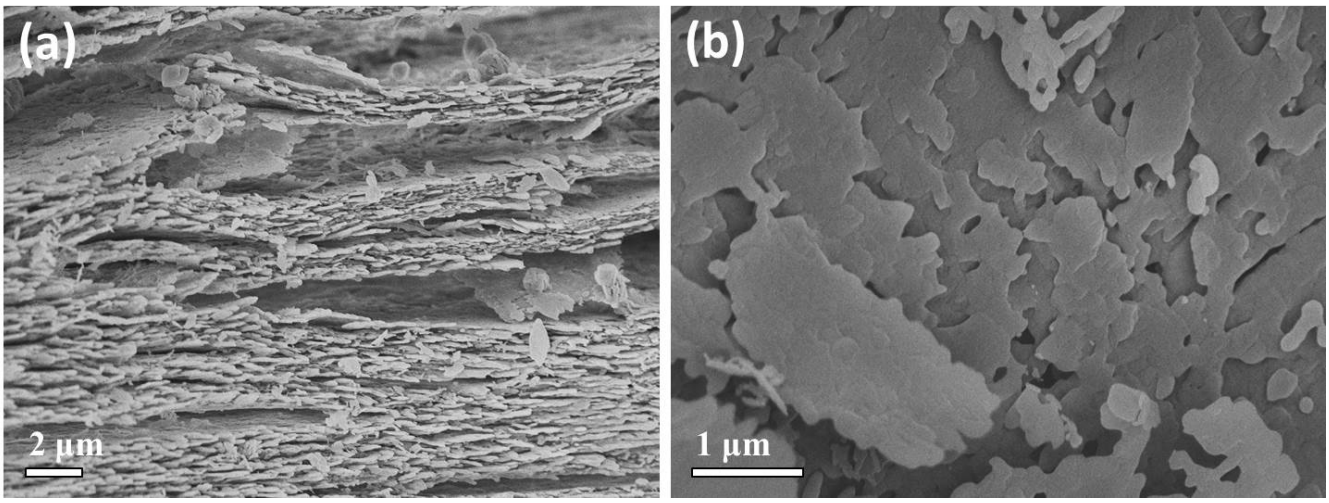

Figure S4. High resolution SEM images of $Zn_5(OH)_8(NO_3)_2 \bullet 2H_2O$/BDC layered composite particles in the 6 h sample with a (a) profile view and (b) top view.

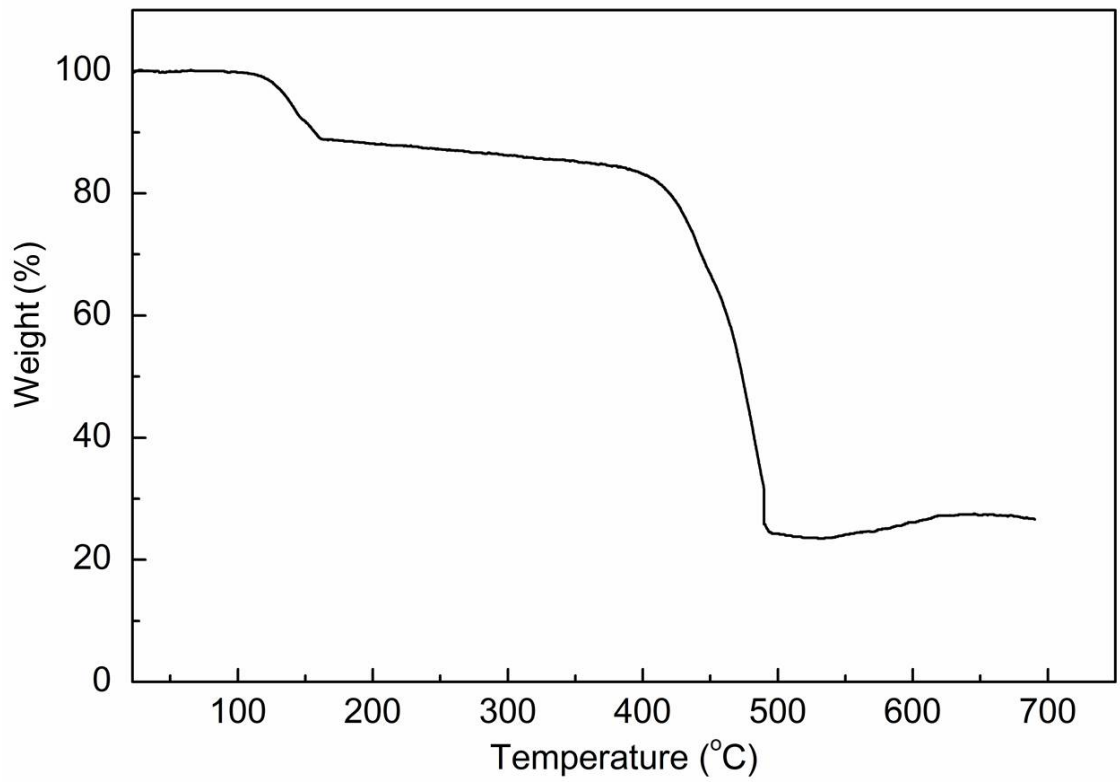

Figure S5. TGA of the 4 h sample showing three distinct changes in weight. On the basis of TGA the composition of the solid phase is calculated as $Zn_5(OH)_8(NO_3)_2 \bullet 2H_2O \bullet 5.89$BDC where BDC is 1,4-benzenedicarboxylic acid. The first weight loss of 10.0 % between 100-170°C is due to the removal of NO_3^-, the second mass loss of 7.0 % between 170-410°C corresponds to the desorption of H_2O from $Zn_5(OH)_8 \bullet 2H_2O \bullet 5.49$BDC whilst the final weight loss of 57.6 % occurring at 410-500°C is due to the decomposition of 1,4-BDC molecules. At temperatures above 500°C the decomposition to ZnO is complete.

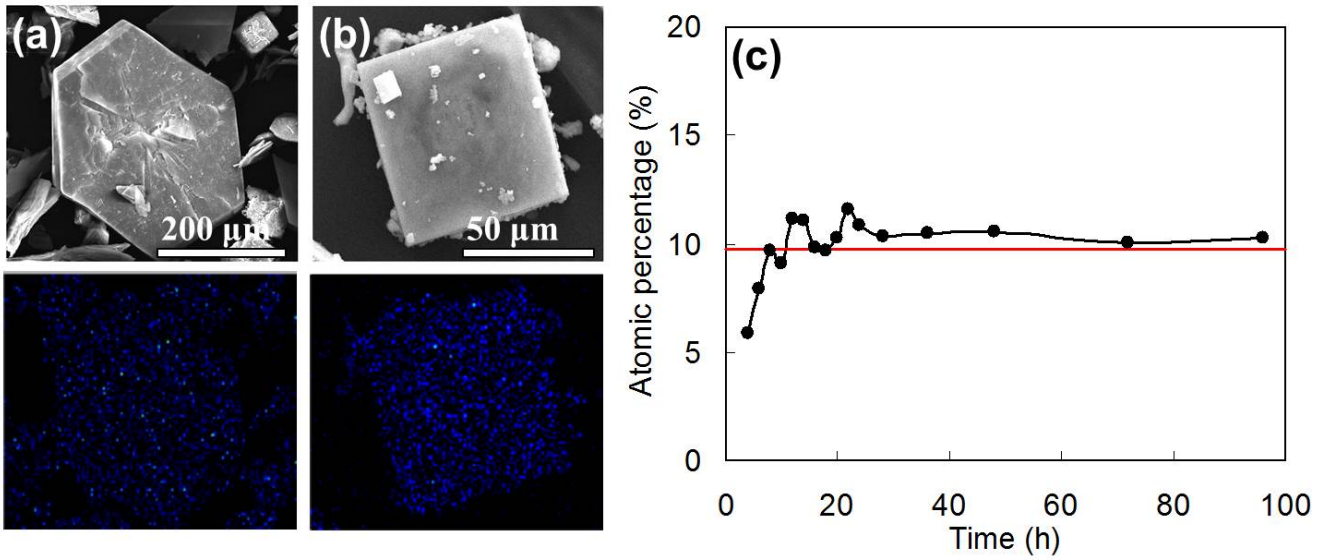

Figure S6. Compositional analysis of specimens at different growth stages. (a,b) EDX mapping of $Zn_5(OH)_8(NO_3)_2 \bullet 2H_2O$ and MOF-5 particles from (a) 6 h and (b) 22 h samples, respectively. Top: SEM images and bottom: the corresponding elemental distributions of Zn. (c) Atomic percentages of Zn in the produced samples with the different reaction times. The red line shows the atomic percentage of Zn in MOF-5 (H is not considered).

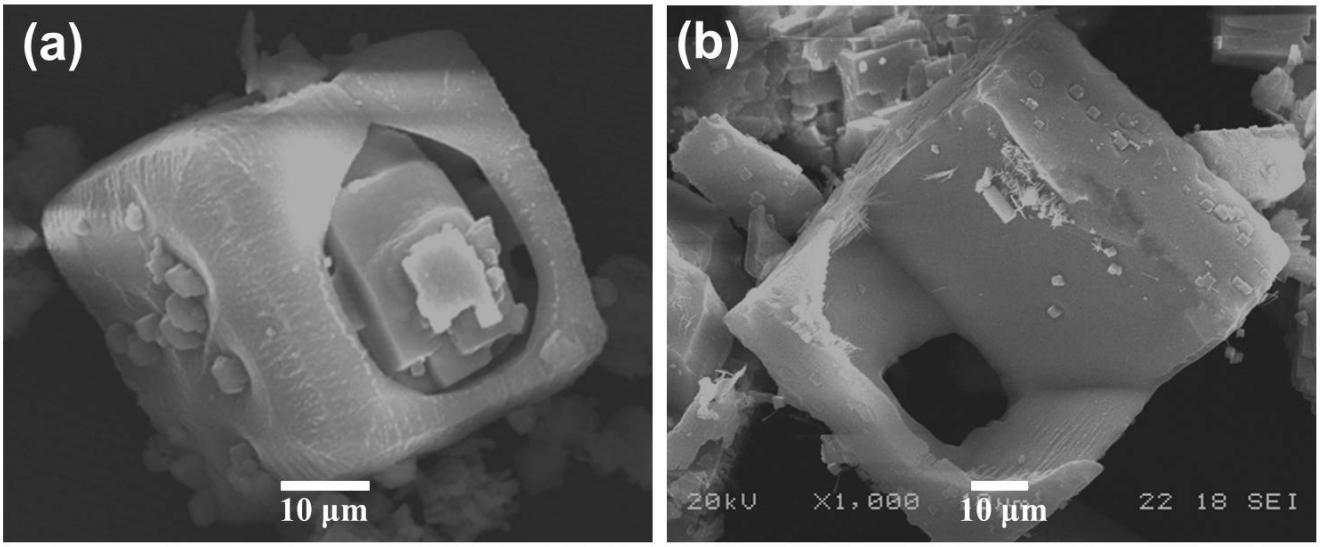

Figure S7. SEM images of broken MOF-5 microcubes. The images were obtained from the (a) 20 h and (b) 22 h samples, showing (a) a core-shell structure and (b) a fragment of a shell after the core crystals were removed.

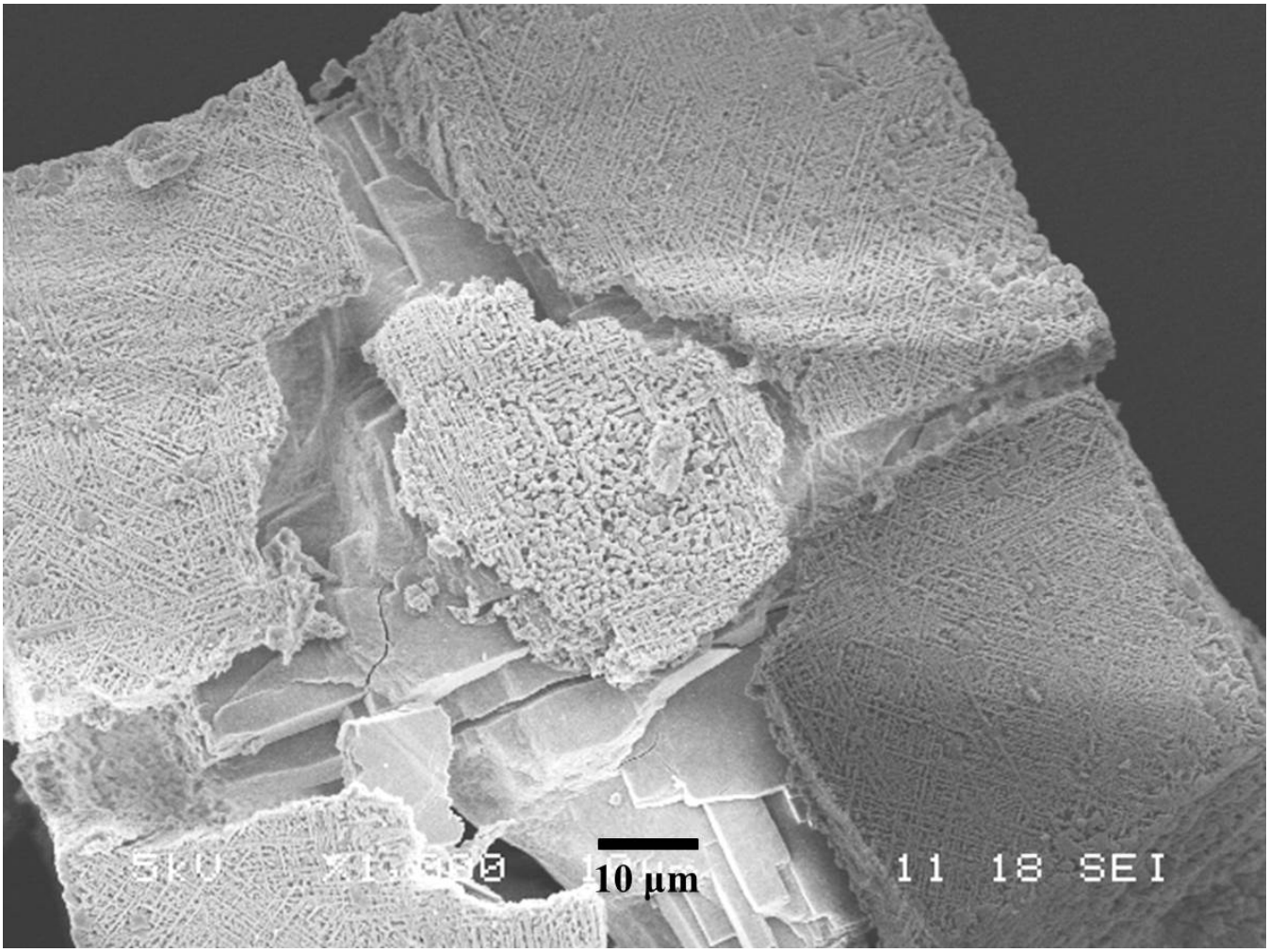

Figure S8. SEM image of a broken cube in the 18 h sample with a textured coating layer. The underneath single crystal surface is exposed.